

---

---

# Dual-Time-Point $^{18}\text{F}$ -FDG PET for the Evaluation of Gallbladder Carcinoma

Yoshihiro Nishiyama, MD<sup>1</sup>; Yuka Yamamoto, MD<sup>1</sup>; Kotaro Fukunaga, MD<sup>1</sup>; Naruhide Kimura, MD<sup>1</sup>; Akihiro Miki, RT<sup>1</sup>; Yasuhiro Sasakawa, RT<sup>1</sup>; Hisao Wakabayashi, MD<sup>2</sup>; Katashi Satoh, MD<sup>1</sup>; and Motoomi Ohkawa, MD<sup>1</sup>

<sup>1</sup>Department of Radiology, Faculty of Medicine, Kagawa University, Kagawa, Japan; and <sup>2</sup>First Department of Surgery, Faculty of Medicine, Kagawa University, Kagawa, Japan

---

Conventional imaging techniques such as ultrasonography, CT, and MRI are able to detect gallbladder abnormalities but are not always able to differentiate a malignancy from other disease processes such as cholecystitis. The purpose of the present study was to evaluate the efficacy of dual-time-point  $^{18}\text{F}$ -FDG PET for differentiating malignant from benign gallbladder disease.

**Methods:** The study evaluated 32 patients who were suspected of having gallbladder tumors.  $^{18}\text{F}$ -FDG PET (whole body) was performed at  $62 \pm 8$  min (early) after  $^{18}\text{F}$ -FDG injection and was repeated  $146 \pm 14$  min (delayed) after injection only in the abdominal region. We evaluated the  $^{18}\text{F}$ -FDG uptake both visually and semiquantitatively. Semiquantitative analysis using the standardized uptake value (SUV) was performed for both early and delayed images (SUV<sub>early</sub> and SUV<sub>delayed</sub>, respectively). The retention index (RI) was calculated according to the equation  $(\text{SUV}_{\text{delayed}} - \text{SUV}_{\text{early}}) \times 100 / \text{SUV}_{\text{early}}$ . The tumor-to-liver ratio was also calculated. **Results:** The final diagnosis was gallbladder carcinoma in 23 patients and benign disease in 9 patients. For visual analysis of gallbladder carcinoma, delayed  $^{18}\text{F}$ -FDG PET images improved the specificity of diagnosis in 2 patients. When an SUV<sub>early</sub> of 4.5, SUV<sub>delayed</sub> of 2.9, and RI of  $-8$  were chosen as arbitrary cutoffs for differentiating between malignant and benign conditions, sensitivity increased from 82.6% to 95.7% and 100% for delayed imaging and combined early and delayed imaging (i.e., RI), respectively. With the same criteria, specificity decreased from 55.6% to 44.4% for delayed imaging and combined early and delayed imaging, respectively. The specificity of  $^{18}\text{F}$ -FDG PET improved to 80% in the group with a normal level of C-reactive protein (CRP) and decreased to 0% in the group with an elevated CRP level. For gallbladder carcinoma, both SUV and tumor-to-liver ratios derived from delayed images were significantly higher than the ratios derived from early images ( $P < 0.0001$ ). **Conclusion:** Delayed  $^{18}\text{F}$ -FDG PET is more helpful than early  $^{18}\text{F}$ -FDG PET for evaluating malignant lesions because of increased lesion uptake and increased lesion-to-background contrast. However, the diagnostic performance of  $^{18}\text{F}$ -FDG PET depends on CRP levels.

**Key Words:** delayed PET;  $^{18}\text{F}$ -FDG PET; gallbladder tumor

**J Nucl Med 2006; 47:633–638**

**G**allbladder carcinoma is the most common malignancy of the biliary system (1,2). Early diagnosis of gallbladder carcinoma remains difficult because of the nonspecificity of its clinical manifestations. The ideal treatment for gallbladder carcinoma is curative surgical resection. When confined to the gallbladder, the tumor can easily be resected, but the tumor usually is not detected until it reaches an advanced stage that has extended beyond the gallbladder (1–3). Accurate preoperative evaluation of gallbladder tumors is essential for curative resection. The usual imaging modalities, such as ultrasonography, CT, and MRI, are able to detect abnormalities of the gallbladder but are not always able to differentiate a malignancy from another disease process such as chronic cholecystitis or adenomyomatosis (4–6).

$^{18}\text{F}$ -FDG PET is a well-established functional imaging technique for diagnostic oncologic imaging that provides information about glucose metabolism in lesions (7). A few studies have evaluated the use of  $^{18}\text{F}$ -FDG PET in the assessment of biliary system tumors (8–10), and even fewer studies have evaluated its use in gallbladder carcinoma (11,12). Furthermore,  $^{18}\text{F}$ -FDG is not tumor specific. This tracer can accumulate in inflammatory lesions and results in low specificity for  $^{18}\text{F}$ -FDG PET in the differentiation of malignant tumors from benign lesions (13).

PET usually is performed 1 h after  $^{18}\text{F}$ -FDG administration. In animal experiments,  $^{18}\text{F}$ -FDG accumulation in tumors constantly increases during 2 or 3 h (14). Conversely, Yamada et al. (15) reported that  $^{18}\text{F}$ -FDG uptake in inflammatory lesions peaked at approximately 1 h after the injection. Some human studies have shown that delayed PET may help in differentiating malignant lesions from benign ones (16–19).

The purpose of the present study was to evaluate whether  $^{18}\text{F}$ -FDG PET is more helpful than the usual imaging modalities in differentiating malignant lesions from benign gallbladder lesions and whether obtaining delayed  $^{18}\text{F}$ -FDG PET images can improve the accuracy of the technique.

---

Received Nov. 14, 2005; revision accepted Jan. 3, 2006.

For correspondence or reprints contact: Yoshihiro Nishiyama, MD, Department of Radiology, Faculty of Medicine, Kagawa University, 1750-1 Ikenobe, Miki-cho, Kita-gun, Kagawa 761-0793, Japan.

E-mail: nisyosi@kms.ac.jp

## MATERIALS AND METHODS

### Patients

Written informed consent was obtained from each patient. The research study protocol was approved by the University Hospital Institution Review Board.

Thirty-two consecutive patients with gallbladder carcinoma suspected on the basis of conventional radiologic studies (12 men and 20 women; mean age, 69.9 y; age range, 34–83 y) and who underwent  $^{18}\text{F}$ -FDG PET between August 2002 and August 2005 were retrospectively selected. Conventional radiologic staging was performed by means of ultrasonography, CT, or MRI. Whenever possible, C-reactive protein (CRP) levels were measured within 2 wk of the PET examination during the routine laboratory work-up.

### $^{18}\text{F}$ -FDG PET Image Acquisition and Reconstruction

All images were acquired using a dedicated PET scanner (ECAT EXACT HR+; Siemens/CTI Inc.). This imaging system enabled the simultaneous acquisition of 63 transverse PET images per field of view. In-plane resolution was 4.6 mm, and axial resolution was 3.5 mm in full width at half maximum. PET scans were acquired in 3-dimensional mode. Transmission scans were obtained using a  $^{68}\text{Ge}$  rod source to generate the attenuation map for attenuation correction. Images were reconstructed with accelerated maximum-likelihood reconstruction and ordered-subset expectation maximization, which reduce image noise and avoid reconstruction artifacts resulting from filtered backprojection reconstruction of data with low-count densities.

Patients were instructed to have no caloric intake for at least 5 h before intravenous administration of  $^{18}\text{F}$ -FDG (3 MBq/kg). Serum glucose concentrations were obtained before the injection. The blood glucose level was less than 200 mg/dL in each patient. A tracer uptake phase of  $62 \pm 8$  min was used, and the patients sat in a quiet room during this phase. After the uptake phase, each patient was placed on the PET scanner table. The PET emission images (early images) were acquired from the proximal thigh to the mid cranium, typically requiring 6–7 bed positions with a 3-min acquisition at each. This acquisition was immediately followed by a transmission scan of the same transverse planes, with a 2-min acquisition at each bed position. Delayed PET emission images of the upper abdomen were acquired at  $146 \pm 14$  min after administration of  $^{18}\text{F}$ -FDG, using 2 or 3 bed positions with a 3-min acquisition at each. This acquisition was immediately followed by a transmission scan of the same transverse planes, using a 2-min acquisition at each bed position.

### PET Image Interpretation and Calculation of Related Parameters

Early and delayed PET images were reviewed on the computer monitor in the transaxial, coronal, and sagittal planes along with maximum-intensity-projection images. Two experienced nuclear medicine physicians independently evaluated  $^{18}\text{F}$ -FDG uptake both visually and semiquantitatively. The evaluating physicians were unaware of the clinical history, except for the results of CT or MRI. The PET images were compared with the corresponding CT or MR images for accurate anatomic identification of the tumor. Any difference of opinion was resolved by consensus.

The degree of  $^{18}\text{F}$ -FDG activity in the tumor was visually scored using a 4-point grading system: no uptake (grade 0), equivocal uptake (grade 1), mildly increased uptake (grade 2), or definitely increased uptake (grade 3). Grade 2 or 3 was considered to represent significant tracer accumulation.

For semiquantitative analysis, a circular region of interest (ROI) was placed over the identified gallbladder lesion and the uninvolved liver using the transverse PET images. For lesions visualized on PET, ROIs were placed over the entire  $^{18}\text{F}$ -FDG-avid lesion, including the largest amount of radioactivity. When little or no lesion-related radioactivity was visually discernible, the ROI was placed at the position of the lesion on CT or MR images. For the liver ROI, a circular 2-cm ROI was placed on a right liver lobe. The standardized uptake value (SUV) was calculated using the following formula:

$$\text{SUV} = c_{\text{dc}} / (d_i / w), \quad \text{Eq. 1}$$

where  $c_{\text{dc}}$  is the decay-corrected tracer tissue concentration (in Bq/g);  $d_i$ , the injected dose (in Bq); and  $w$ , the patient's body weight (in g). The maximal SUV in the lesion ROI and the mean SUV in the liver ROI were calculated for each ROI. Furthermore, we evaluated the change in uptake by the lesion as the retention index (RI) as follows:

$$\text{RI} = (\text{SUV}_{\text{delayed}} - \text{SUV}_{\text{early}}) \times 100 / \text{SUV}_{\text{early}}, \quad \text{Eq. 2}$$

where  $\text{SUV}_{\text{early}}$  is the SUV of the early image and  $\text{SUV}_{\text{delayed}}$  is the SUV of the delayed image. As a contrast value, the tumor-to-liver (T/L) ratio was also calculated by dividing the tumor SUV by the liver SUV. We referred to the T/L ratio of the early image as the T/L(E) ratio and the T/L ratio of the delayed image as the T/L(D) ratio.

### Final Diagnosis

The PET findings were correlated with the results of histologic, clinical, or radiologic follow-up. A hypermetabolic  $^{18}\text{F}$ -FDG lesion was considered true positive for malignant involvement if malignancy was proven by histologic analysis or if the lesion resolved on follow-up PET after therapy or progressed on follow-up PET or other imaging (ultrasonography, CT, or MRI). An  $^{18}\text{F}$ -FDG-negative lesion was considered true negative if its size remained stable on conventional imaging follow-up for at least 6 mo.

### Statistical Analysis

Differences in semiquantitative parameters were analyzed by the Mann-Whitney  $U$  test and the Wilcoxon signed-rank test for unpaired and paired observations, respectively. All semiquantitative data were expressed as mean  $\pm$  SD. For all analyses,  $P$  values of less than 0.05 were considered statistically significant. The final diagnosis was also compared with the PET results, and diagnostic accuracy was determined. For calculation of sensitivity and specificity, the optimal SUV and RI for differentiating between malignant and benign lesions were chosen retrospectively to yield the lowest number of false-negative and false-positive results. For statistical comparison of early and delayed PET, and of groups according to CRP level, the  $\chi^2$  test was used. Significance was assumed if the probability of a first-degree error was less than 0.05 ( $\chi^2 > 3.841$ ).

## RESULTS

Twenty-three lesions (14 based on histologic verification; 9 based on clinical or radiologic follow-up) were gallbladder carcinoma and the remaining 9 (6 based on histologic

verification; 3 based on clinical or radiologic follow-up) were benign gallbladder disease.

Table 1 shows the diagnostic performance of PET for the detection of gallbladder carcinoma visually and using semi-quantitative analysis. Two gallbladder carcinomas (both 8 mm in diameter) were visually identified on delayed PET images but not on early PET images. Two gallbladder carcinomas (both 10 mm in diameter) were not visually identified on either early or delayed PET images. When calculated using visual analysis, sensitivity increased from 82.6% to 91.3% for delayed PET, whereas specificity did not change. Overall, for visual analysis of gallbladder carcinoma, delayed PET improved the specificity of diagnosis in 2 patients (6%). However, diagnostic values did not significantly differ between early and delayed PET images.

When an  $SUV_{early}$  of 4.5,  $SUV_{delayed}$  of 2.9, and RI of  $-8$  were chosen as arbitrary cutoffs for differentiating between malignant and benign conditions, sensitivity increased from 82.6% to 95.7% and 100% for delayed imaging and combined early and delayed imaging (namely RI), respectively, whereas specificity decreased from 55.6% to 44.4% for delayed imaging and combined early and delayed imaging. Overall, diagnosis of gallbladder carcinoma using semiquantitative analysis of PET images was improved for delayed imaging and combined early and delayed imaging—in 3 patients (9%) and 4 patients (13%), respectively. On the other hand, diagnosis was worsened in 1 patient (3%) for both delayed imaging and combined early and delayed imaging, because of visualization of a benign lesion. However, diagnostic values did not significantly differ between early, delayed, and combined early and delayed PET. Figure 1 shows an example of improved visualization of a gallbladder carcinoma on delayed images.

Table 2 shows the diagnostic value of using semiquantitative analysis of  $^{18}F$ -FDG PET images for the detection of gallbladder carcinoma in patients with unknown, normal, or elevated levels of CRP. CRP levels were measured in all patients except patient 2. The specificity of  $SUV_{early}$ ,  $SUV_{delayed}$ , and RI was significantly higher for patients

with normal CRP levels than for those with elevated CRP levels ( $\chi^2 = 4.80$  for each comparison). The sensitivity of  $SUV_{early}$  and  $SUV_{delayed}$  in patients with normal CRP levels was lower than that in patients with elevated CRP levels, but the difference was not statistically significant. The accuracy of  $SUV_{early}$ ,  $SUV_{delayed}$ , and RI in patients with normal CRP levels was higher than that in patients with elevated CRP levels, but the difference was not statistically significant. Figure 2 shows an example of  $^{18}F$ -FDG PET findings for a patient with xanthogranulomatous cholecystitis and elevated CRP.

Table 3 shows the mean values of SUV, T/L ratio, and RI based on semiquantitative analysis of  $^{18}F$ -FDG PET images.  $SUV_{delayed}$ , T/L(D) ratio, and RI significantly differed ( $P < 0.05$ ) between patients with gallbladder carcinoma and patients with benign disease.  $SUV_{early}$  and  $SUV_{delayed}$  significantly differed ( $P < 0.0001$ ) in patients with gallbladder carcinoma but not in patients with benign disease. T/L(E) and T/L(D) ratios significantly differed both in patients with gallbladder carcinoma ( $P < 0.05$ ) and in patients with benign disease ( $P < 0.0001$ ). Normal liver tended to show a lower  $SUV_{delayed}$  than  $SUV_{early}$ , and mean  $SUV_{delayed}$  was significantly lower than mean  $SUV_{early}$  ( $P < 0.0001$ ).

## DISCUSSION

Although a few reports have indicated that  $^{18}F$ -FDG PET has value in the diagnosis of biliary system tumors (8–10), the diagnostic role of this technique for gallbladder carcinoma has not been evaluated fully. In the present study, we found good sensitivity and accuracy for differential diagnosis of gallbladder carcinoma. These results confirmed the ability to detect gallbladder carcinoma using  $^{18}F$ -FDG PET. However, benign inflammatory gallbladder lesions can also accumulate  $^{18}F$ -FDG and result in false-positive interpretations of PET studies.

Koh et al. (11) reported that the sensitivity of  $^{18}F$ -FDG PET was 75% for the diagnosis of gallbladder carcinoma.

**TABLE 1**  
Diagnostic Value of  $^{18}F$ -FDG PET Using Visual and Semiquantitative Analysis in 32 Patients Suspected of Having Gallbladder Carcinoma

Parameter	Visual analysis		Semiquantitative analysis		
	Early image	Delayed image	$SUV_{early}$	$SUV_{delayed}$	RI
Sensitivity	82.6% (19/23)	91.3% (21/23)	82.6% (19/23)	95.7% (22/23)	100% (23/23)
Specificity	44.4% (4/9)	44.4% (4/9)	55.6% (5/9)	44.4% (4/9)	44.4% (4/9)
PPV	79.2% (19/24)	80.8% (21/26)	82.6% (19/23)	81.5% (22/27)	82.1% (23/28)
NPV	50.0% (4/8)	66.7% (4/6)	55.6% (5/9)	80.0% (4/5)	100% (4/4)
Accuracy	71.9% (23/32)	78.1% (25/32)	75.0% (24/32)	81.3% (26/32)	84.4% (27/32)

PPV = positive predictive value; NPV = negative predictive value.

Numbers in parentheses indicate numbers of patients.  $SUV_{early}$  cutoff value was 4.50;  $SUV_{delayed}$  cutoff value was 2.90; RI cutoff value was  $-8$ .

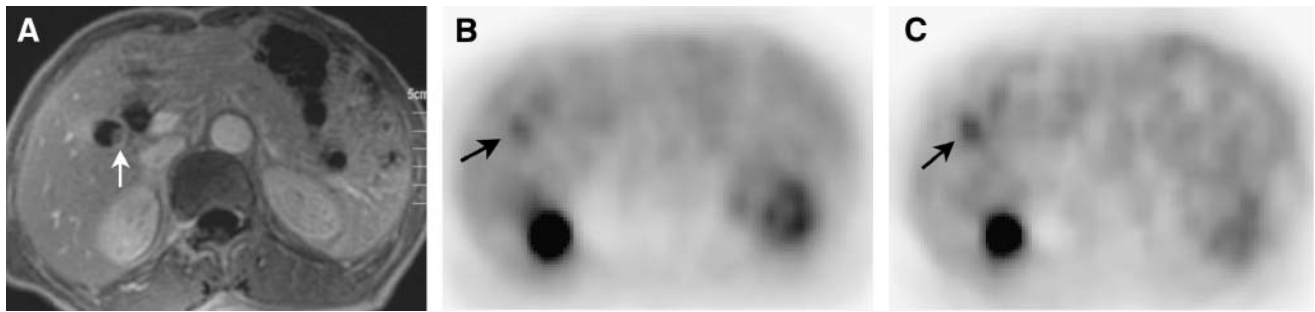


**FIGURE 1.** Radiologic findings in 66-y-old man with gallbladder carcinoma. (A) MR image shows small polypoid lesion projecting into lumen of gallbladder (arrow). (B) Early  $^{18}\text{F}$ -FDG PET image ( $\text{SUV}_{\text{early}}$ , 2.72; T/L(E) ratio, 1.10) shows slightly increased uptake at tumor site (arrow). (C) Delayed  $^{18}\text{F}$ -FDG PET image ( $\text{SUV}_{\text{delayed}}$ , 3.21; T/L(D) ratio, 1.52) shows more definite uptake (arrow) than does early image. CRP was 0.25 mg/dL.

Rodriguez-Fernandez et al. (12) reported a sensitivity of 80% for this modality. The sensitivity of  $^{18}\text{F}$ -FDG PET in the present study was 82%–100% for the diagnosis of gallbladder carcinoma. Our best cutoff SUVs and RI values for the calculation of sensitivity and specificity were slightly higher than the mean values for normal liver and much lower than the mean values for benign disease, possibly because of the small number of patients in our study. Further studies involving a larger number of patients are required to determine the appropriate cutoff values. We performed both early and delayed PET. Although they did not significantly differ in diagnostic performance, a 6.3% difference was observed visually for the same lesions. Also, a 9%–13% difference was observed on semiquantitative analysis. This effect was semiquantitatively demonstrated by a statistically significant increase in SUV and T/L ratio. The higher contrast resolution, which provides a better lesion-to-background ratio, facilitates visual detection. The usefulness of dual-time-point PET has previously been reported for various tumors (16–20). However, to our knowledge, no reports have described dual-time-point PET of gallbladder carcinoma.

Although the number of patients studied was small, our preliminary results show that delayed PET is more sensi-

tive than early PET for detecting gallbladder carcinoma. Reinhardt et al. (21) reported that delayed  $^{18}\text{F}$ -FDG PET was highly accurate in the detection of malignancy in the liver hilus, although they evaluated only delayed PET.

Although delayed PET was more sensitive than early PET for the detection of gallbladder carcinoma, some false-negative findings also occurred. Two gallbladder carcinomas 10 mm in diameter were not visualized even on delayed imaging. The limited sensitivity of PET for small lesions may have several causes. Activity in small lesions may be underestimated because of the partial-volume effect, movement artifacts caused by nongated breath holding, or physiologic liver  $^{18}\text{F}$ -FDG uptake. These factors illustrate the intrinsic limitations of PET resolution for small lesions even if delayed images are acquired. In patients with mucinous adenocarcinoma of the gallbladder, a false-negative result has also been reported, probably secondary to poor cellular density (12). However, in the present study, false-negative PET findings occurred for patients with tubular adenocarcinoma and not mucinous adenocarcinoma.

Several studies have reported that malignant disease showed a higher SUV on delayed images than on early images—that is to say, malignancy yields positive RI values (16–19). On the other hand, benign disease showed a lower

**TABLE 2**  
Diagnostic Value of  $^{18}\text{F}$ -FDG PET Using Semiquantitative Analysis in 32 Patients Suspected of Having Gallbladder Carcinoma with Unknown, Normal, and Elevated Levels of CRP

Parameter	C-reactive protein level								
	Unknown			Normal (<1.0 mg/dL)			Elevated ( $\geq 1.0$ mg/dL)		
	$\text{SUV}_{\text{early}}$	$\text{SUV}_{\text{delayed}}$	RI	$\text{SUV}_{\text{early}}$	$\text{SUV}_{\text{delayed}}$	RI	$\text{SUV}_{\text{early}}$	$\text{SUV}_{\text{delayed}}$	RI
Sensitivity	100% (1/1)	100% (1/1)	100% (1/1)	73.3% (11/15)	93.3% (14/15)	100% (15/15)	100% (7/7)	100% (7/7)	100% (7/7)
Specificity	100% (1/1)	0% (0/1)	0% (0/1)	80%* (4/5)	80%* (4/5)	80%* (4/5)	0% (0/3)	0% (0/3)	0% (0/3)
Accuracy	100% (2/2)	50% (1/2)	50% (1/2)	75% (15/20)	90% (18/20)	95% (19/20)	70% (7/10)	70% (7/10)	70% (7/10)

\* $P < 0.05$  compared with elevated-level group ( $\chi^2$  test).

Numbers in parentheses indicate numbers of patients.  $\text{SUV}_{\text{early}}$  cutoff value was 4.50;  $\text{SUV}_{\text{delayed}}$  cutoff value was 2.90; RI cutoff value was  $-8$ .

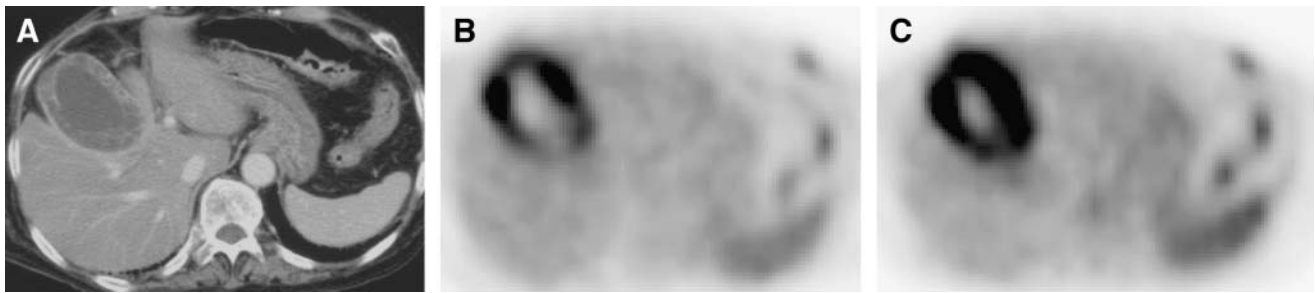


**FIGURE 2.** Radiologic findings in 68-y-old woman with xanthogranulomatous cholecystitis. (A) CT image obtained after administration of contrast material shows thickening and enhancement of gallbladder wall. (B) Early  $^{18}\text{F}$ -FDG PET image (SUV<sub>early</sub>, 8.39; T/L(E) ratio, 3.18) shows intense uptake at gallbladder lesion. (C) Delayed  $^{18}\text{F}$ -FDG PET image (SUV<sub>delayed</sub>, 10.90; T/L(D) ratio, 4.74) shows more definite uptake than does early image. CRP was 9.34 mg/dL.

SUV on delayed images than on early images—that is to say, benignancy yields negative RI values. In the present study, all but 2 gallbladder carcinomas showed positive RI values. However, benign disease also showed positive RI values in 6 of 9 patients. Patients with acute inflammation may have false-positive results even if delayed PET is additionally performed. In the present study, the CRP level was more than 1 mg/dL at the time of PET in all patients with false-positive findings. Although the sensitivity of combined early and delayed PET (i.e., RI) was slightly higher than that of delayed PET, the accuracy of these parameters did not significantly differ. Specificity did not change for combined early and delayed PET. Although the number of patients studied was small, this observation suggests that only delayed PET may be sufficient to reduce imaging time in busy clinical settings.

$^{18}\text{F}$ -FDG is taken up not only by tumor cells but also by activated inflammatory cells (13–15). In most patients presenting with chronic cholecystitis, inflammatory cells are few and, typically, do not show increased  $^{18}\text{F}$ -FDG uptake. Nevertheless, in some patients with chronic cholecystitis, acute episodes of cholecystitis develop, such as elevated CRP, white blood cell counts, proinflammatory cytokines, or abdominal pain. The specificity in the present study was low. One cause of reduced specificity was thought to be the acute inflammatory condition. We also evaluated the correlation between elevated CRP levels and  $^{18}\text{F}$ -FDG uptake in gallbladder lesions, because the systemic response of patients to acute cholecys-

titis can be assessed using CRP levels (22). The specificity of PET improved to 80% in the group with normal CRP levels. On the other hand, the specificity of PET decreased to 0% in the group with elevated CRP levels. These results suggest that diagnostic difficulties may occur in patients with elevated CRP levels. CRP is a better predictor of the specificity of PET. Our results illustrate the relationship between the severity of inflammation and the specificity of PET. We also should consider the possibility of concomitant inflammatory processes in gallbladder cancer. The CRP results therefore stress the importance of proper patient selection. Not only CRP but also other clinical or laboratory data emphasizing the existence of acute inflammatory conditions might be helpful in this respect. A PET examination should be recommended for patients with nonacute inflammation, such as those with normal CRP levels, to differentiate malignant lesions from benign lesions.

## CONCLUSION

The results of the present study demonstrate the feasibility and clinical potential of  $^{18}\text{F}$ -FDG PET for differential diagnosis of gallbladder carcinoma. Delayed  $^{18}\text{F}$ -FDG PET was more helpful than early  $^{18}\text{F}$ -FDG PET in the evaluation of malignancy, because of the increased uptake by lesions and the increased lesion-to-background contrast. In order to minimize false-positive findings, patients with signs of acute inflammation should be excluded from examination.

**TABLE 3**  
Semiquantitative Analysis of  $^{18}\text{F}$ -FDG PET in 32 Patients Suspected of Having Gallbladder Carcinoma

Condition	Early image		Delayed image		RI
	SUV <sub>early</sub>	T/L(E) ratio	SUV <sub>delayed</sub>	T/L(D) ratio	
Gallbladder carcinoma	7.35 ± 3.71	2.40 ± 1.15	9.30 ± 4.98*†	3.54 ± 1.73*†	24.62 ± 13.00*
Benign disease	5.40 ± 3.44	1.70 ± 1.00	6.27 ± 5.02	2.22 ± 1.61‡	7.32 ± 21.29
Normal liver	3.05 ± 0.46		2.63 ± 0.48†		-13.63 ± 5.99

\* $P < 0.05$  compared with benign disease (Mann-Whitney  $U$  test).

† $P < 0.0001$  compared with early image (Wilcoxon signed-rank test).

‡ $P < 0.05$  compared with early image (Wilcoxon signed-rank test).

Values are mean ± SD.

## REFERENCES

1. Nevin JE, Moran TJ, Kay S, et al. Carcinoma of the gallbladder: staging, treatment, and prognosis. *Cancer*. 1976;37:141–148.
2. Roberts JW, Daugherty SF. Primary carcinoma of the gallbladder. *Surg Clin North Am*. 1986;66:743–749.
3. De Aretxabala X, Roa I, Burgos L, et al. Gallbladder cancer in Chile: a report on 54 potentially resectable tumours. *Cancer*. 1992;69:60–65.
4. Gore RM, Yaghami V, Newmark GM, et al. Imaging benign and malignant disease of the gallbladder. *Radiol Clin North Am*. 2002;40:1307–1323.
5. Grand D, Horton KM, Fishman E. CT of the gallbladder: spectrum of disease. *AJR*. 2004;183:163–170.
6. Yoshimitsu K, Honda H, Aibe H, et al. Radiologic diagnosis of adenomyomatosis of gallbladder: comparative study among MRI, helical CT, and transabdominal US. *J Comput Assist Tomogr*. 2001;25:843–850.
7. Coleman RE. Clinical PET in oncology. *Clin Positron Imaging*. 1998;1:15–30.
8. Anderson CD, Rice MH, Pinson W, et al. Fluorodeoxyglucose PET imaging in the evaluation of gallbladder carcinoma and cholangioma. *J Gastrointest Surg*. 2004;8:90–97.
9. Kluge R, Schmidt F, Caca K, et al. Positron emission tomography with [<sup>18</sup>F]fluoro-2-deoxy-D-glucose for diagnosis and staging of bile duct cancer. *Hepatology*. 2001;33:1029–1035.
10. Kato T, Tsukamoto E, Kuge Y, et al. Clinical role of <sup>18</sup>F-FDG PET for initial staging of patients with extrahepatic bile duct cancer. *Eur J Nucl Med Mol Imaging*. 2002;29:1047–1054.
11. Koh T, Taniguchi H, Yamaguchi A, et al. Differential diagnosis of gallbladder cancer using positron emission tomography with fluorine-18-labeled fluoro-deoxyglucose (FDG-PET). *J Surg Oncol*. 2003;84:74–81.
12. Rodriguez-Fernandez A, Gomez-Rio M, Llamas-Elvira JM, et al. Positron-emission tomography with fluorine-18-fluoro-2-deoxy-D-glucose for gallbladder cancer diagnosis. *Am J Surg*. 2004;188:171–175.
13. Kubota R, Yamada S, Kubota K, et al. Intratumoral distribution of fluorine-18-fluorodeoxyglucose in vivo: high accumulation in macrophages and granulation tissues studied by microautoradiography. *J Nucl Med*. 1992;33:1972–1980.
14. Zhuang H, Pourdehnad M, Lambright ES, et al. Dual time point <sup>18</sup>F-FDG PET imaging for differentiating malignant from inflammatory processes. *J Nucl Med*. 2001;42:1412–1417.
15. Yamada S, Kubota K, Kubota R, et al. High accumulation of fluorine-18-fluorodeoxyglucose in turpentine-induced inflammatory tissue. *J Nucl Med*. 1995;36:1301–1306.
16. Nakamoto Y, Higashi T, Sakahara H, et al. Delayed <sup>18</sup>F-fluoro-2-deoxy-D-glucose positron emission tomography scan for differentiation between malignant and benign lesions in the pancreas. *Cancer*. 2000;89:2547–2554.
17. Matthies A, Hickeyson M, Cuchiara A, et al. Dual time point <sup>18</sup>F-FDG PET for the evaluation of pulmonary nodules. *J Nucl Med*. 2002;43:871–875.
18. Demura Y, Tsuchida T, Ishizaki T, et al. <sup>18</sup>F-FDG accumulation with PET for differentiation between benign and malignant lesions in the thorax. *J Nucl Med*. 2003;44:540–548.
19. Nishiyama Y, Yamamoto Y, Monden T, et al. Evaluation of delayed additional FDG PET imaging in patients with pancreatic tumour. *Nucl Med Commun*. 2005;26:895–901.
20. Kubota K, Itoh M, Ozaki K, et al. Advantage of delayed whole-body FDG-PET imaging for tumour detection. *Eur J Nucl Med*. 2001;28:696–703.
21. Reinhardt MJ, Strunk H, Gerhardt T, et al. Detection of Klatskin's tumor in extrahepatic bile duct strictures using delayed <sup>18</sup>F-FDG PET/CT: preliminary results for 22 patient studies. *J Nucl Med*. 2005;46:1158–1163.
22. Diederichs CG, Staib L, Glasbrenner B, et al. F-18 fluorodeoxyglucose (FDG) and C-reactive protein (CRP). *Clin Positron Imaging*. 1999;2:131–136.